World Engineering & Applied Sciences Journal 1 (1): 09-17, 2010
ISSN 2079-2204

An Effective and Safe Charging Algorithm for Lead-Acid Batteries in PV Systems

Abd El-Shafy A. Nafeh

Electronics Research Institute, Cairo, Egypt

Abstract: In this paper a new charging algorithm is proposed to charge lead-acid batteries in photovoltaic (PV) systems. This algorithm can return discharged lead-acid batteries to their 100% state of charge (SOC) quickly and at the same time can avoid the associated problems of the excessive gassing phenomenon at overcharge. The proposed algorithm can be applied in the PV systems by using a DC-DC converter, which differs from the traditional on/off regulators in that it can not only be used to charge the battery and protects it from overcharging, but it can also be used to quickly and safely charge the battery to 100% SOC through better exploitation of the available PV energy. The simulation results verify that, by using the proposed algorithm, the discharged battery can always restore its 100% SOC compared to the conventional charging algorithms.

Key words: PV system % Battery charging % State of charge % DC-DC converter % Maximum-power-point tracking

INTRODUCTION

Lead-acid batteries provide the most common means of energy storage in photovoltaic (PV) systems today. Where, the prominent feature of their operation, in these systems, is cycling, which means that the batteries are recharged after the occurrence of a discharging condition. Therefore, designing of a good charger is the ultimate goal of the PV researchers; since, the effectiveness and high efficiency of the battery charger can affect the battery life and maintenance requirements which must be allowed for in the design of the PV system [1-7].

Various common types of battery chargers are available that fulfill the charging role and at the same time protect the batteries against the overcharging condition. The simplest battery charger is the self-regulator [1, 3], which is used in small systems and constructed, simply, through the direct connection of the battery with the PV array via a blocking diode. This configuration relies on the correct choice of the operating point of the PV array, to match the battery charging requirements [1] and can not be standardized easily because it depends on the implementation (wiring) and is very sensitive to the temperature effect [3].

In small and medium applications, a shunt regulator [1, 3, 4] can be used to dissipate the unwanted power, which overcharges the batteries, from the PV array. The common implementation of the shunt regulator is to use a transistor in parallel with the PV array, which is set to conduct and divert excess PV current from the battery at a certain threshold voltage value.

In large applications, the battery is disconnected from the PV array by means of a series regulator [1, 3, 4]. This can be an electromechanical switch (for example, a relay) or a solid-state device (bipolar transistor, MOSFET, etc.). The former devices have the advantages that they do not dissipate energy but their reliability can be a problem in locations with high dust or sand occurrence.

Due to the nonlinear current-voltage characteristics of the PV array and the unpredictable variation of these characteristics with insolation level and cell temperature, also due to the variation of the battery terminal voltage with its state of charge (SOC), the previous common types of battery chargers can not always operate the PV array at its corresponding maximum-power points (MPPs). Alternatively, DC-DC converters [8-11] can provide the battery, continuously, with the maximum-power obtainable from the PV array, whenever possible; which is very desirable and necessary in most PV applications. Moreover, the DC-DC converters can be controlled to protect the battery against the overcharging conditions, which is needed to prolong the battery life [3, 8-11].

In this paper a new charging algorithm is proposed and applied, to a proposed battery charging system, by using the capabilities of the DC-DC converters in PV systems, to quickly and safely charge lead-acid batteries to their 100% SOC.

Corresponding Author: Abd El-Shafy A. Nafeh, Electronics Research Institute, Cairo, Egypt

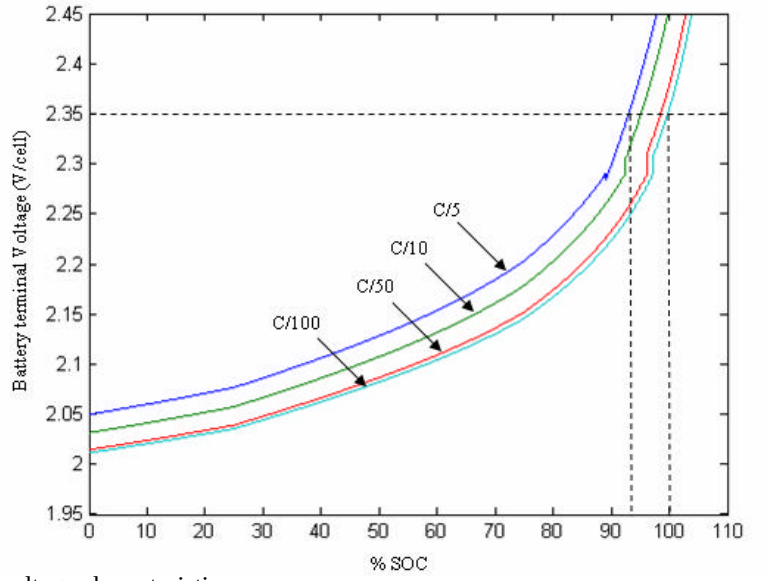

Fig. 1: Typical charge voltage characteristics

Lead-acid Batteries: In simplified terms, the lead-acid battery comprises two electrodes of lead (-ve plate) and lead dioxide (+ve plate) and the electrolyte of sulphuric acid diluted with water. In practical construction, the electrodes are formed by a lead grid (sometimes alloyed with calcium or antimony) carrying the active material in the form of a porous structure that offers a large surface area for chemical reactions with the electrolyte. The chemical reactions that take place during battery operation are:

- During the discharging process, lead-sulphate is formed at both electrodes and sulphuric acid is removed from the electrolyte (i.e., it becomes weaker).
- During the charging process, lead dioxide is formed at the +ve electrode, pure lead is formed at the-ve electrode and sulphuric acid is liberated in the electrolyte (i.e., it becomes stronger) [1, 3-5].

Therefore, long periods in a low SOC can cause much larger crystals of lead sulphate to form on the battery plates than the small crystals which normally form during discharge. This process, known as sulphation, leads to loss of capacity and reduces battery life; since the formation of large lead-sulphate crystals at the plates hinders the reversible chemical reactions.

Figure 1 illustrates the charge voltage curves, of the used lead-acid battery [3], as a function of the battery's SOC for different charging rates. This figure indicates that the charge voltage, generally, increases with both increasing SOC and increasing charge rate.

At the beginning of the charging process, the charge voltage normally increases with increasing SOC. After a relatively slow increase, in voltage, up to about 2.35 V/cell, the conventional end of charge voltage is reached and electrolysis or gassing begins (i.e., the conversion of water into hydrogen and oxygen gases at the-ve and +ve electrodes, respectively). When the terminal voltage starts to climb rapidly at near 100% SOC, excessive gassing and loss of electrolyte take place. This overcharging can produce corrosion of the +ve grids and can cause the active material of the plates to loosen and flake off by the accompanying excessive gassing. Also, it may increase the battery temperature to the point of being destructive to the plates and separators. Moreover, it increases the need for maintenance and represents a safety hazard. Therefore, overcharging the battery can reduce its capacity and life. Whereas, in moderate levels, the gassing process can be used to advantage by alleviating stratification of the electrolyte. Where, the battery operation tends to favor a non-uniform electrolyte distribution such that the electrolyte with the highest density occurs at the bottom of the battery vessel. This stratification of the electrolyte promotes corrosion and sulphation of the bottom part of the-ve electrode, but can be avoided by a regular weak overcharge in which gassing is used to stir the electrolyte [1, 3-5].

Charging Algorithm: The most common method of regulation and control of lead-acid batteries is based on the approximate SOC measurement via battery terminal

Table 1: End of charge voltages at the various charging rates.

Charge rate (A)	MPP operation (C/5 to C/10)	C/20	C/30	C/40	C/50	C/100
End of charge voltage (V/cell)	2.34	2.342	2.344	2.346	2.348	2.35

voltage. This method restricts the conventional end of charge voltage to about 2.35 V/cell, as indicated in Fig. 1. Where, by using this method the batteries can not always be fully charged to 100% SOC; this is because the previously mentioned voltage value is chosen to restrict the amount of gassing, at the same time makes the battery approaches 100% SOC as large as possible. In this way, the battery will always remain in a low charge state for extended periods of time, which leads to the occurrence of a sulphation phenomenon. This sulphation can be avoided, in conventional methods, by bringing all batteries up to 100% SOC regularly (using an 'equalization charge') and by minimizing the time of exposure to low SOC conditions. The equalizing charge or overcharge, which should be carried out once a month or more depending on the battery state, ensures that weaker cells in the battery have the opportunity to become fully charged. Although, overcharging the battery is good for short periods as means of charge equalization and to prevent stratification of the electrolyte, it is not good over prolonged periods due to the problems of the excessive gassing. It is to be noted that the gassing process, for lead-acid batteries, begins when the terminal voltage of the battery reaches about 2.3 V/cell, irrespective of the charge rate and the quantity of gas formed depends on the portion of current not absorbed by the battery. Therefore, to maintain the battery capacity and at the same time to extend the battery life, batteries are kept at near 100% of their full charge or returned to that state quickly after a partial or deep discharge. The following charging algorithm is suggested to charge the lead-acid batteries quickly and safely to their full charge. This algorithm aims to avoid the sulphation phenomenon of the batteries (by bringing all the battery cells to 100% SOC quickly) and to restrict the amount of gassing such that the electrolyte stratification and at the same time the excessive gassing problems are avoided. A more careful examination of Fig. 1 suggests that an even better charging algorithm might be to initially charge the battery at a relatively high rate that corresponds to the MPP operation of the PV array (i.e., from C/5 to C/10, where C is the battery capacity in ampere-hours). When the terminal voltage of the battery at that rate reaches 2.34 V/cell at 25 °C (with a temperature compensation of-1 mV/°C/cell [3]), the charging rate is then successively decreased in steps, starting from C/20 to C/100, until the battery ultimately reaches 100% SOC at the charging rate C/100 (Fig. 1). The used charging rates, in this work and the corresponding end of charge voltages at 25°C are indicated in Table 1.

Configuration of the Charging System: The proposed block diagram of the battery charging system is shown in Fig. 2. This system consists mainly of four components, which are the PV array, the DC-DC converter, the lead-acid battery and the control system.

In this work, the two important components that are necessary to achieve the proposed charging algorithm are the DC-DC converter and the control system. Therefore, this work will clarify these two components only. The PV array and battery are previously modeled and clarified in details in [12] and they are considered, in this work, to be only as the power generating source and the DC load, respectively.

The Dc-dc Converter: As the name implies, the DC-DC converter converts directly from DC to DC and is also known as a DC chopper. Like a transformer, it can be used to step-down or step-up a DC voltage source [13, 14].

In most PV applications, the DC-DC converters [8-11, 15] are commonly used as matching converters that adjust the operating point of the system to the MPP of the PV array. The step-down converter (i.e., the buck converter) can be used to drive a low voltage load from a high voltage PV array and it can operate efficiently at any insolation level. Therefore, the utilization of the buck converter in PV applications, that contain lower voltage batteries, is highly recommendable. Here, the DC-DC converter, of Fig. 3, is not only used to track the MPP of the PV array at all insolation levels and cell temperatures, but also used to safely charge the lead-acid battery from the PV array to 100% SOC; by adjusting its switching duty cycle D through controlling the pulse-width modulation (PWM) control signal.

The dynamic model of the used step-down converter can be derived as

$$\frac{d}{dt}\begin{bmatrix} V_{PV} \\ i_L \end{bmatrix} = \begin{bmatrix} 0 & 0 \\ \frac{D}{L} & 0 \end{bmatrix}\begin{bmatrix} V_{PV} \\ i_L \end{bmatrix} + \begin{bmatrix} \frac{1}{C_1} & -\frac{D}{C_1} & 0 \\ 0 & 0 & -\frac{1}{L} \end{bmatrix}\begin{bmatrix} I_{PV} \\ I_B \\ V_B \end{bmatrix}$$

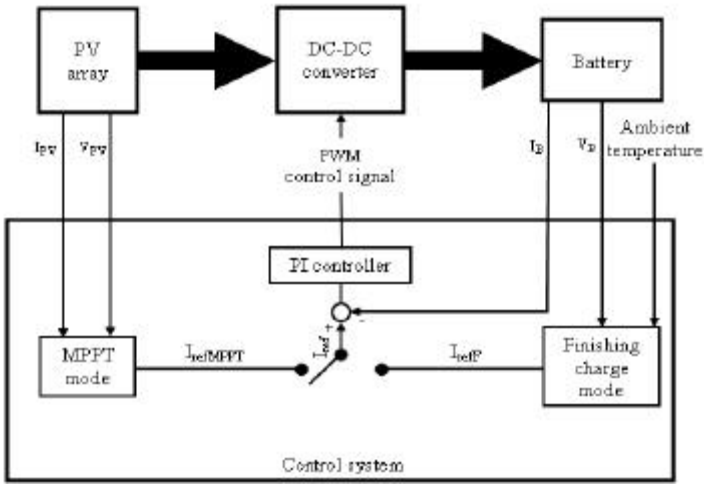

Fig. 2: Block diagram of the battery charging system

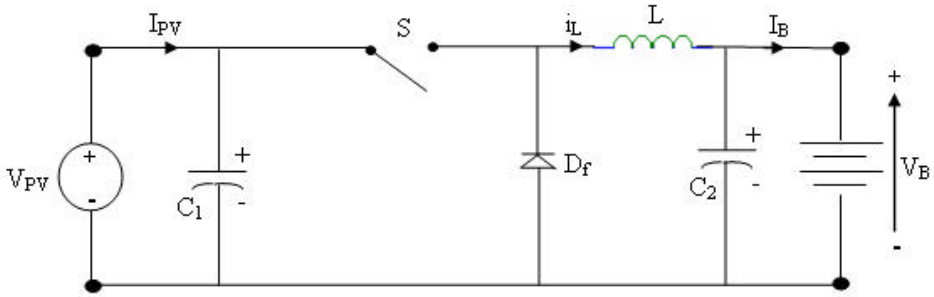

Fig. 3: The step-down DC-DC converter

The Control System: The PWM control signal or simply the control signal is produced, from the control system, due to the action of the PI controller. This signal can adjust the duty cycle of the DC-DC converter, which in turn can adjust the converter input characteristics to extract the desired power from the PV array and transferring it to the battery. The desired power extracted from the PV array is controlled, in this work, by adjusting the desired (i.e., reference) battery current I_{ref}; since the battery voltage is considered to be constant for small interval of time.

The control system comprises two control modes that are responsible to produce the battery reference current. These modes are the maximum-power-point tracking (MPPT) control mode and the finishing charge control mode. Such that the MPPT reference current $I_{refMPPT}$ is used, at first, to effectively charge the battery from its low SOC to the end of charge voltage 2.34 V/cell, at the high charging rate that is ranged from C/5 to C/10 and produced from the MPPT of the PV array. Afterwards, the finishing charge reference current I_{refF} is utilized to safely finalize the charging process of the battery to 100% SOC. Therefore, by using the two consecutive control signals of the control system, the lead-acid battery could be quickly and safely charged to 100% SOC.

The MPPT Mode: This control mode is based on using the perturb and observe (P andO) peak-power tracker (PPT) [9, 15, 16], which operates by periodically incrementing or decrementing the array current. If a given perturbation leads to an increase (decrease) in array power, the next perturbation is made in the same (opposite) direction. Thus, the peak-power tracker continuously hunts or seeks peak-power current.

The flowchart of this mode is indicated in Fig. 4. Where, k is the current sampling instant of the array current I_{PV}, voltage V_{PV} and power P_{PV}.

The Finishing Charge Mode: The finishing charge mode is carried out, in this work, through decreasing the charging rate of the battery in successive steps (i.e., from C/20 to C/100, as indicated in Table 1) until the battery

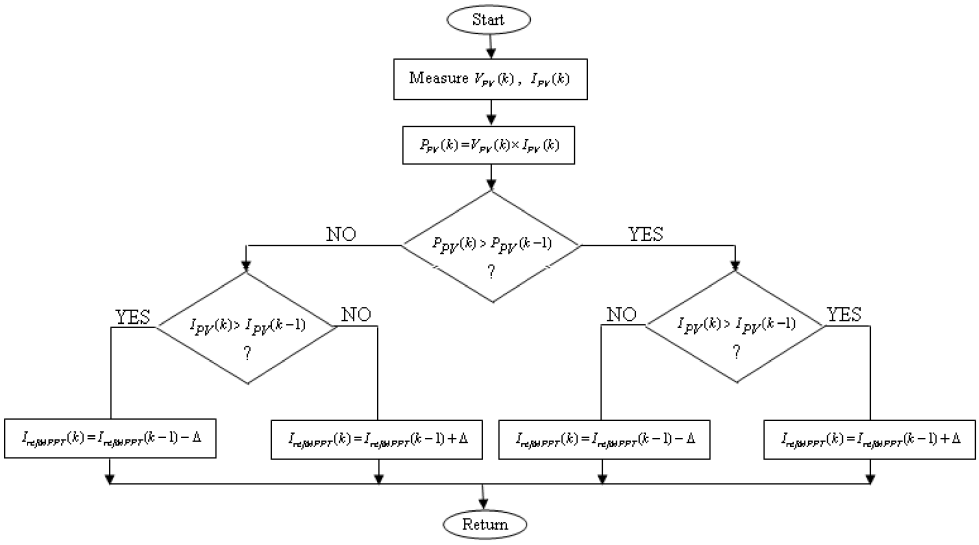

Fig. 4: Flowchart of the P andO PPT

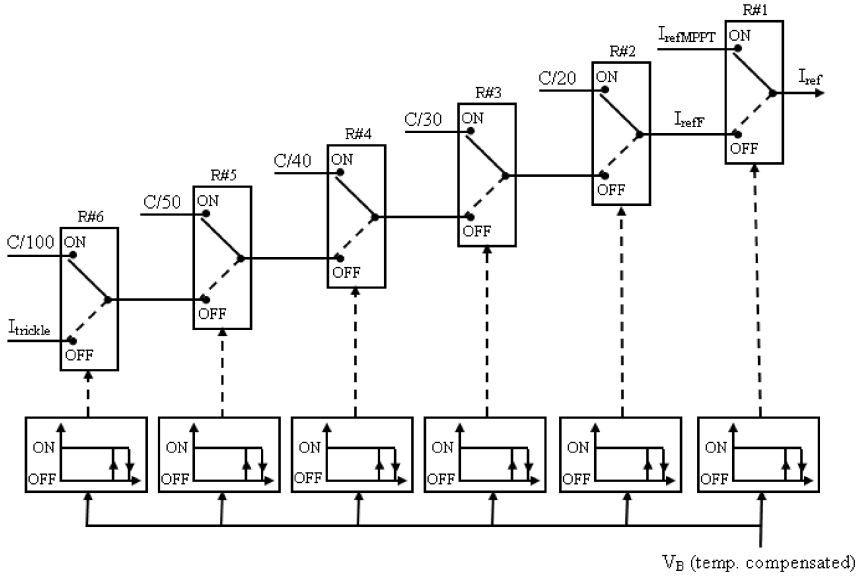

Fig. 5: Achievement of the finishing charge mode.

ultimately reaches 100% SOC, which corresponds to the end of charge voltage of 2.35 V/cell at the final charging rate C/100.

The finishing charge mode is achieved, in this work, with the help of six-series-connected relays that are driven using comparators with hysterics, as illustrated in Fig. 5. The interconnection of the six relays is such that the output connection of a certain relay is connected to the turn off connection of the previous relay and the corresponding charging rate, of the considered relay, is connected to its turn on connection. Also, the output connection of the first relay (i.e., R#1) is connected to the battery reference current, whereas the turn off connection of the final relay (i.e., R#6) is connected to the battery trickle current $I_{trickle}$. Note, here, that the switch off point of a certain relay is set to the end of charge voltage that corresponds to the charging rate connected to the relay's turn on connection (Table 1), whereas its turn on point is set to equal the battery minimum voltage V_{Bmin}. In this way, when a certain relay is disconnected at its corresponding end of charge voltage, it remains switched off and will not switch on again until the battery has discharged somewhat to a voltage value corresponding to V_{Bmin}. Thus, the possible oscillatory process of all relays, resulted due to the battery internal resistance, can be overcome.

Figure 5 illustrates that when the lead-acid battery undergoes a charging process from a low SOC, the battery reference current will equal, at first, to $I_{refMPPT}$. Such that, when the battery is charged, using the array MPP current, to a voltage value of 2.34 V/cell, the battery reference current will then decrease successively in steps from C/20 to C/30 to C/40 to C/50 and finally to C/100. Afterwards, when the battery is fully charged to 100% SOC, which corresponds to battery voltage of 2.35 V/cell at the final charging rate of C/100, the battery reference current will set to $I_{trickle}$; to compensate for the control system power consumption and the battery self-discharge rate. Note that $I_{trickle}$ was set to 0 A, in this work.

RESULTS AND DISCUSSION

The proposed PV/Battery charging system was simulated, in this work, by using MATLAB/SIMULINK, to achieve the ultimate goals of the new charging algorithm.

In order to investigate the capability of the new charging algorithm with the aid of the DC-DC converter, relative to the commonly used one, in operating the PV array at its MPPs and in safely charging the lead-acid battery to 100% SOC, the performance of the control system and that of the battery must be recorded at different environmental conditions. The variation of the environmental conditions during the charging time is shown in Fig. 6; such that the variation of the insolation level and that of the ambient temperature are shown in Figs. 6(a) and (b), respectively.

Figure 7 indicates the output control signal of the proposed charging system relative to that of the conventional charging one. These control signals are utilized in both cases, through PWM, to control the DC-DC converter to charge the battery with the available array maximum power. When the value of these two signals become zero, as indicated in the later portion of Fig. 7, this means that the charging process is finished and the corresponding battery is completely charged to the corresponding specified limit. In addition, it is indicated, also from Fig. 7, that the control signal of the proposed system has only a prolonged portion of time, due to the existence of the finishing charge mode.

Figures 8(a), (b), and (c) show, respectively, the performance of the battery current, voltage and power by using the proposed and conventional systems. These three figures indicate that the corresponding battery charging currents, voltages and powers of the two systems are the same during the charging portion of the conventional system, while they significantly differ in the prolonged charging time of the proposed system. And this is due to the existence of the extra finishing charge mode in the proposed system and, also, due to the fact that the conventional charging system is commonly designed to end the charging process (at the MPPT charging rate) at a specified end of charge voltage limit (. 2.35 V/cell); to avoid the excessive gassing phenomenon associated with battery charging. In addition, Fig. 8 (a) illustrates that during the MPPT mode of the two systems, the battery charging currents are proportional to the solar insolation level. While, during

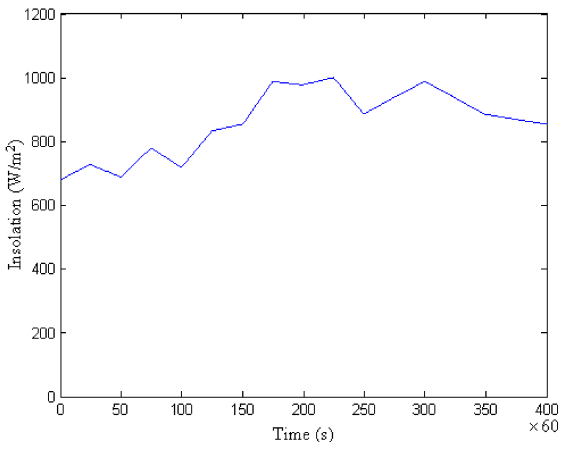

(a) Variation of insolation level

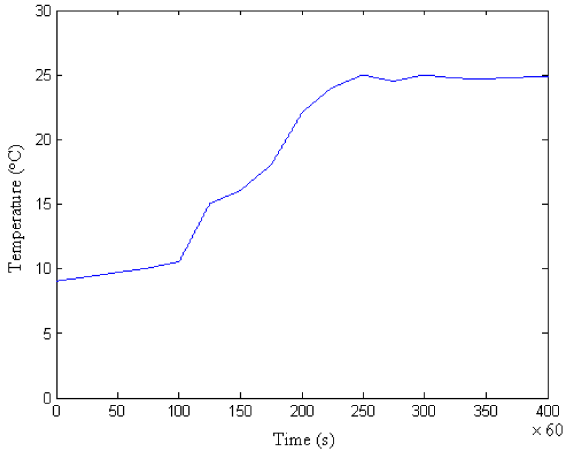

(b) Variation of ambient temperature

Fig. 6 Variation of the environmental conditions during the charging time.

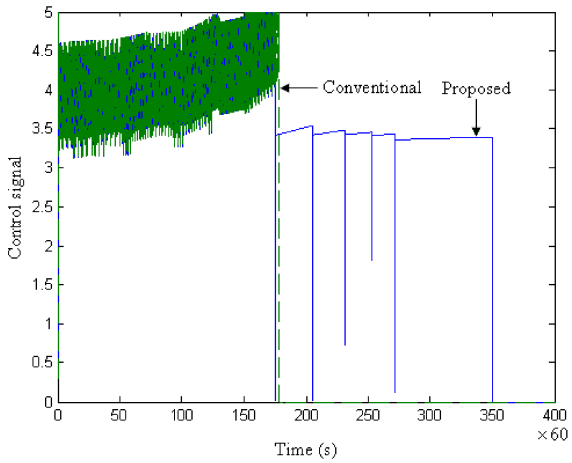

Fig. 7: Control signal during the charging time

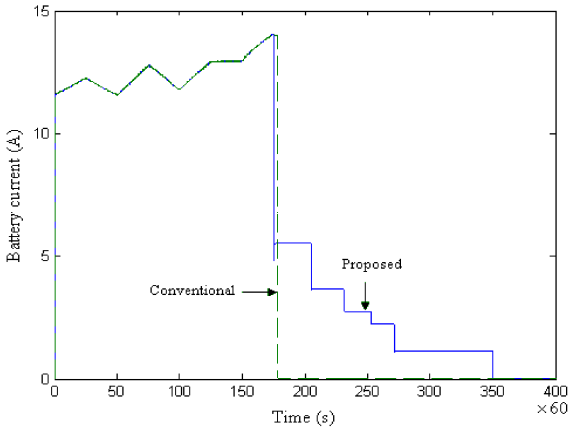

(a) Performance of the battery current

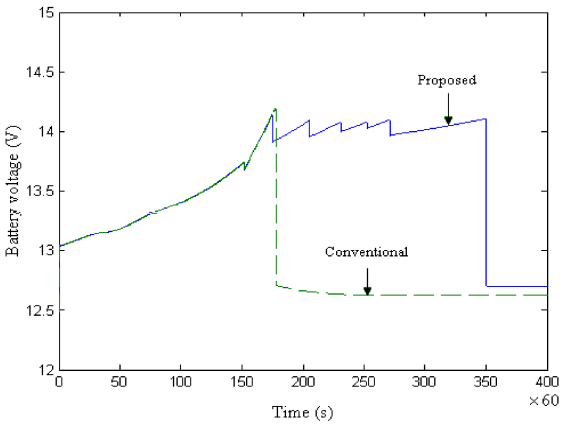

(b) Performance of the battery voltage

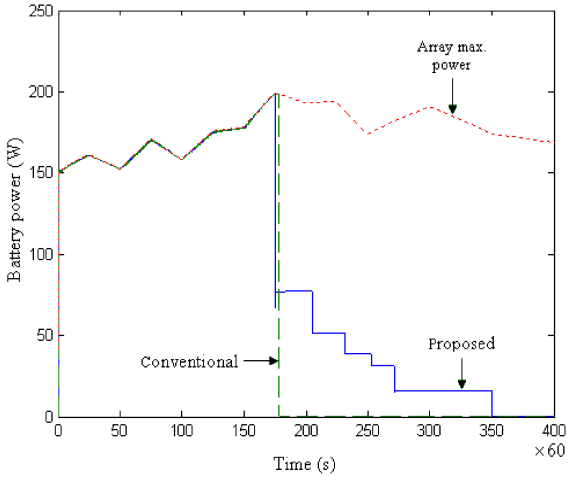

(c) Performance of the battery power

Fig. 8: Performance of the battery current, voltage and power during the charging time.

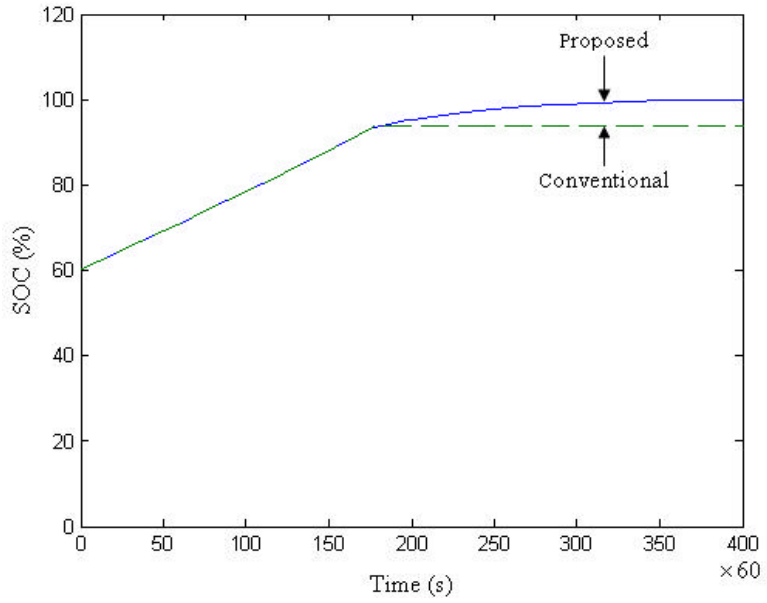

Fig. 9: Performance of the battery SOC during the charging time

the finishing charge mode of the proposed system, the battery current of the conventional system is 0 A and that of the proposed system decreases successively in steps to reach 0 A when the battery is fully charged. Also, Fig. 8 (b) indicates that during the MPPT mode of the two systems, the battery voltages are effectively increased with the corresponding charging currents (i.e., MPPT charging rates). While, during the finishing charge mode of the proposed system, the battery voltage of the conventional system drops to its open-circuit value (described at the corresponding battery final SOC) and that of the proposed system is switched to increase slowly and safely with the corresponding specified charging rates till the battery is fully charged; it, then, drops to its open-circuit value that corresponds to the battery final SOC. Moreover, Fig. 8(c) shows that during the MPPT mode of the two systems, the two system batteries are effectively charged with the corresponding array maximum powers. While, during the finishing charge mode of the proposed system, the battery power of the conventional system is 0 W and that of the proposed system decreases successively in steps to reach 0 W when the battery is fully charged (i.e., as the corresponding battery current).

Figure 9 is dedicated for the evaluation of the performance of the battery SOC by using the proposed system compared to the conventional one. Thus, it is seen from this figure that the proposed system can ultimately charge the battery to about 100% SOC, while the conventional system can ultimately charge the same battery to only about 93.6% SOC.

CONCLUSIONS

A new charging algorithm, which uses the capabilities of the DC-DC converters in PV systems, is proposed and applied to a proposed PV/Battery charging system, to quickly and safely charge lead-acid batteries to their 100% SOC. The proposed algorithm is based on using two modes: the MPPT mode and the finishing charge mode. The function of the MPPT mode, which is based on using the P andO PPT, is to effectively charge the lead-acid battery (quickly and safely) to about 90-95% SOC; whereas that of the finishing charge mode, which is based on using a set of series-connected relays, is to fully charge the battery (safely) to about 100% SOC. Therefore, the proposed algorithm can ensure: (a) a better exploitation of the available PV power, by operating the PV array at its MPPs; and (b) an increased battery lifetime, by restoring the SOC of all battery cells (including the weaker cells) to their 100% SOC quickly and safely. Simulation results indicated that by using the proposed (two mode) charging algorithm, the discharged lead-acid battery can ultimately restore its 100% SOC quickly and safely. Whereas, on the other hand, the conventional charging algorithm can ultimately charge the lead-acid battery to only about 93.6% SOC.

REFERENCES

1. Markvart, T., 1994. Solar Electricity. New York: John Wiley and Sons.
2. Luque, A. and S. Hegedus, 2003. Handbook of Photovoltaic Science and Engineering. Chichester, England: John Wiley and Sons, Ltd, pp: 753.
3. Lasnier, F. and T.G. Ang, 1990. Photovoltaic Engineering Handbook. Bristol, England: IOP Publishing Ltd.
4. Green, M.A., 1982. Solar Cells, Operating Principles, Technology and System Applications. N. J.: Prentice-Hall Inc., Englewood Cliffs.
5. Messenger, R. and J. Ventre, 2000. Photovoltaic Systems Engineering. Boca Raton, Florida, USA: CRC Press LLC.
6. O'Connor, J.A., 2009. Simple Switchmode Lead-Acid Battery Charger. Unitrode Application Note, Texas Instruments Inc., pp: 226-234. [Online]. Available: http://focus.ti.com/lit/an/slua055/slua055.pdf
7. Li, C., X. Zhu, G. Cao, S. Sui and M. Hu, 2009. Dynamic Modeling and Sizing Optimization of Stand-Alone Photovoltaic Power Systems Using Hybrid Energy Storage Technology. Renewable Energy, 34: 815-826.
8. Koutroulis, E., K. Kalaitzakis and N.C. Voulgaris, 2001. Development of a Microcontroller-Based, Photovoltaic Maximum Power Point Tracking Control System. IEEE Trans. Power Electron., 16(1): 46-54.
9. Hua, C.C. and P.K. Ku, 2005. Implementation of a Stand-Alone Photovoltaic Lighting System with MPPT, Battery Charger and High Brightness LEDs. In the Proceedings of the 6th IEEE Int'l Conf. on Power Electronics and Drive Systems (PEDS), vol. 2, Kuala Lumpur, Malaysia, pp: 1601-1605.
10. Koutroulis, E. and K. Kalaitzakis, 2004. Novel Battery Regulation System for Photovoltaic Applications. IEE Proc.-Electr. Power Appl., 151(2): 191-197.
11. Hou, C.L., J. Wu, M. Zhang, J.M. Yang and J.P. Li, 2004. Application of Adaptive Algorithm of Solar Cell Battery Charger. In the Proceedings of the IEEE Int'l Conf. on Electric Utility Deregulation, Restructuring and Power Technologies (DRPT2004), Hong Kong, pp: 810-813.
12. Abd El-Shafy A. Nafeh, 2009. An Optimum Control Strategy for Energy Management in a Remote Area Stand-Alone PV System. Open Renewable Energy Journal, 2: 91-98.
13. Rashid, M.H., 2004. Power Electronics Circuits, Devices and Applications. Upper Saddle River, N. J.: 3rd ed, Pearson Prentice Hall.
14. Roman, E., R. Alonso, P. Ibanez, S. Elorduizapatarietxe and D. Goitia, 2006. Intelligent PV Module for Grid-Connected PV Systems. IEEE Trans. Ind. Electron., 53(4): 1066-1073.
15. Jiang, J.A., T.L. Huang, Y.T. Hsiao and C.H. Chen, 2005. Maximum Power Tracking for Photovoltaic Power Systems. Tamkang J. Sci. Engineering, 8(2): 147-153.
16. Kuo, Y., T. Liang and J. Chen, 2001. Novel Maximum-Power-Point-Tracking Controller for Photovoltaic Energy Conversion System. IEEE Trans. Ind. Electron., 48(3): 594-601.